

## PERFORMANCE OF WEAK-BEAM, STRONG-COLUMN RC FRAMES STRENGTHENED AT THE JOINTS BY FRP\*

S. A. HADIGHEH<sup>1</sup>, MAHMOUD R. MAHERI<sup>2\*\*</sup> AND S. S. MAHINI<sup>3</sup>

<sup>1</sup>School of Civil, Environmental and Chemical Engineering, RMIT University, Melbourne, Australia

<sup>2</sup>Dept. of Civil Engineering, Shiraz University, Shiraz, I. R. of Iran

Email: maheri@shirazu.ac.ir

<sup>3</sup>Dept. of Civil and Environmental Engineering, The University of New England, Armidale, NSW 2351, Australia

**Abstract**– Despite the large volume of work reported on the behaviour of reinforced concrete joints, only a few studies have been carried out to investigate the influence of retrofitting joints by FRP composites on the overall behaviour of an RC frame. To study the seismic performance of Moment Resisting RC frames retrofitted at joints by FRP, experimental and numerical investigations are carried out on a scaled-down frame of weak-beam, strong-column type, retrofitted by applying the FRP laminates at the web of the joints. Representing constitutive models are used to introduce the behaviour of concrete, steel and fibre-reinforced polymers in the numerical investigation. Full post-peak behaviour of the joints is captured considering strain softening of concrete. Finite element results show good agreement with the experimental findings. It is found that the maximum load carrying and displacement capacities of the joint after strengthening are increased and that the first steel yielding and development of crack occur at higher loads, further away from the joint, into the beam. The effects of different values of fracture energies on the behaviour of the reinforced concrete joint are also investigated. Nonlinear pushover analyses are also carried out to predict the seismic performance of an eight-storey and two additional low-rise frames retrofitted by steel braces and FRP. It is shown that by using FRP laminates at the web of the joints, the stiffness, the behaviour factor,  $R$ , performance level and the lateral load-carrying capacity of the damaged/plain frame are markedly increased.

**Keywords**– Reinforced concrete frames, joints, fibre-reinforced polymers, plastic hinge, pushover analysis, ductility,  $r$  factor, performance levels

### 1. INTRODUCTION

A large number of reinforced concrete structures which were designed according to old codes, do not satisfy the seismic design requirements of the new codes. Over the last three decades many techniques such as steel [1, 2] or concrete [3] jacketing have been proposed to strengthen deficient RC structures. However, heavy weight, low workability and low resistance against erosion, have rendered these techniques somewhat unpopular. After the Anchorage earthquake in Alaska, the San Fernando earthquake in the US and the Managua earthquake in Nicaragua, epoxy resin was used extensively to retrofit damaged existing RC structures [4, 5]. Although the results showed that using epoxy resins could restore the strength, stiffness and energy-dissipation capacity of the structure, such techniques can only be used for structures with low levels of damage.

During the 1990s, the idea of using composite materials to retrofit RC frames was developed. Varastehpour and Hamelin [6] conducted some experiments on three beams which had been strengthened with FRP layers. They showed that FRP retrofitting can increase the ultimate moment capacity and reduce

\*Received by the editors June 1, 2011; Accepted July 14, 2012.

\*\*Corresponding author

the ultimate curvature of beams. Kachlakev and McCurry [7] as well as other researchers [8-10], showed that FRP can increase the load carrying capacity of beams up to 150%.

Li et al. [11] carried out some experiments on reinforced concrete beam-column connections which were wrapped with hybrid FRP sheets. Their experiments showed that stiffness and load-carrying capacity of joints were improved. Also, Mosallam [12], Parvin and Granata [13,14], Said and Nehdi [15], Mukherjee and Joshi [16], and Parvin and Wu [17] have noted that strengthening of connections can increase the moment capacity, ductility, initial stiffness, energy dissipation capacity and reduce joint rotations and stresses in both concrete and reinforcement. Experiments conducted by Parvin and Wu [17] showed that this technique can also prevent a brittle shear failure. Mahini and Ronagh [18, 19] proposed a new method in strengthening of exterior beam-column connections. The proposed method was to stick carbon FRP sheets of specific lengths to the sides of the beams of a reinforced concrete joint (i.e. web-bonded FRP). Mahini and Ronagh [18, 19] tested seven scaled-down plain/FRP-retrofitted RC exterior joints of a typical Ordinary Moment Resisting Frame under monotonic/cyclic loads. Their tests results showed that the method is effective and capable of upgrading the strength of the system and also, can relocate the plastic hinge formation away from the face of the column.

Balsamo et al. [20] investigated the behaviour of a full-scale, 4-storey frame with shear walls. The FRP strengthened frame was subjected to pseudo dynamic loads. By retrofitting the frame, not only the local but also the global stability was improved. In addition, displacement and rotational capacities of joints were enhanced without any loss of strength. Zou et al. [21] investigated a 3-storey frame which was strengthened with FRP around its columns. They observed that strengthening could increase the strength of columns with only marginal increase on their stiffness. Reduced stiffness is, however, suitable for the overall stability of the frame as stiffer columns lead to higher seismic forces. In addition, the failure mode of the frame was changed from a column side-sway mechanism to an acceptable storey deformation level with weak beam-strong column behaviour. Mahini et al. [22] and Niroomandi et al. [23] assessed performance of an FRP-retrofitted RC moment resisting frame and compared the result with those of the same frame retrofitted with steel braces. In their research, moment-rotation relationship of RC joints retrofitted with CFRP web-bonded developed by Mahini and Ronagh [18] were obtained using the ANSYS software [19]. They showed that the performance level and the seismic behaviour factor of the FRP retrofitted RC frame are improved or even significantly enhanced in comparison with the original frame and are comparable with those of the steel braced frame. As a full post-peak behaviour is difficult to obtain using ANSYS, in their study Mahini et al. [22] and Niroomandi et al. [23] decided to concentrate on the peak strength of plain/retrofitted joints. Mostofinejad and Talaeitaba, on the other hand, developed FE models using ANSYS software to analyse beam-column connections strengthened at flanges by FRP [24]. They reported good ductility and strength enhancement for the connection due to this retrofitting scheme.

In this research, the numerical model of an exterior joint of an eight-storey building that was tested under monotonic loads by Mahini and Ronagh [18] is first simulated in ABAQUS [25] finite element software before and after web bonding by CFRP layers and is verified against the experimental model [18, 26]. The ABAQUS nonlinear numerical analyses were then carried out on all the other joints of the eight-storey frame studied by Mahini and Ronagh [18], and the full post-peak moment-curvature curve for each individual joint of the frame before retrofitting and after retrofitting by FRP were evaluated. The moment-curvature data evaluated for each joint using ABAQUS software were then incorporated into SAP2000 [27] models of the full 8-storey frame so that nonlinear pushover analyses of the original and the retrofitted frames could be carried out and their performances evaluated and compared. Also, based on Maheri and Ghaffarzadeh's research [28], two additional low-rise frames rehabilitated earlier with steel braces, are retrofitted at joints by FRP laminates and their performances are also compared.

## 2. EXPERIMENTAL DATA

In an earlier experimental study, Mahini and Ronagh [18] investigated the behaviour of an RC joint before and after strengthening at web by FRP. The joint was a 1:2.2 scaled down joint, selected from an eight-storey residential RC building (Fig. 1).

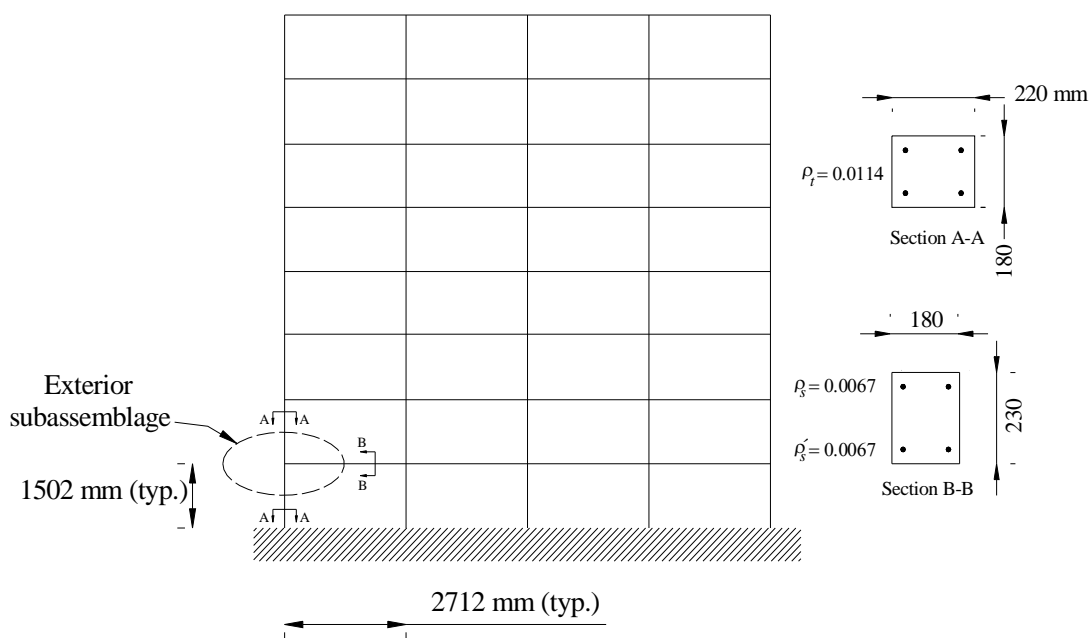


Fig. 1. Prototype eight-story building

The frame was designed according to the Australian Concrete Code AS3600 (2001) [29] and as an Ordinary Moment Resisting Frame (OMRF) similar to non-ductile frame based on ACI-318, American Standard [30]. Details of the scaled selected joint are shown in Fig. 2 [18].

Mahini and Ronagh constructed three identical specimens. One specimen (CSM0) was used as a control specimen and the other two specimens (RSM1 and RSM2) were used to investigate the effects of FRP retrofitting. At first, an increasing load was applied to the control specimen at the position shown in Fig. 2. The load control regime was used up to the steel reinforcement yielding and continued using a displacement control regime corresponding to a ductility ratio of 5. At around 17 kN load, flexural cracks developed at the end of the beam and close to the column face. The ultimate load of this specimen was about 24.6 kN with a displacement of 82 mm [18].

The other two specimens were similarly loaded to failure. In order to investigate the influences of FRP web bonding technique on the behaviour of the joint, one and three layers of unidirectional FRP were wrapped over the joint core area and the back of the column of the specimens RSM1 and RSM2, respectively. The number, length and thickness of FRP layers for different specimens are tabulated in Table 1.

Table 1. Geometry of FRP layers [18]

Specimen	$l_f$ (mm)	No. of piles	$t_f$ (mm)
CSM0	-	0	-
RSM1	350	1	0.165
RSM2	200	3	0.495

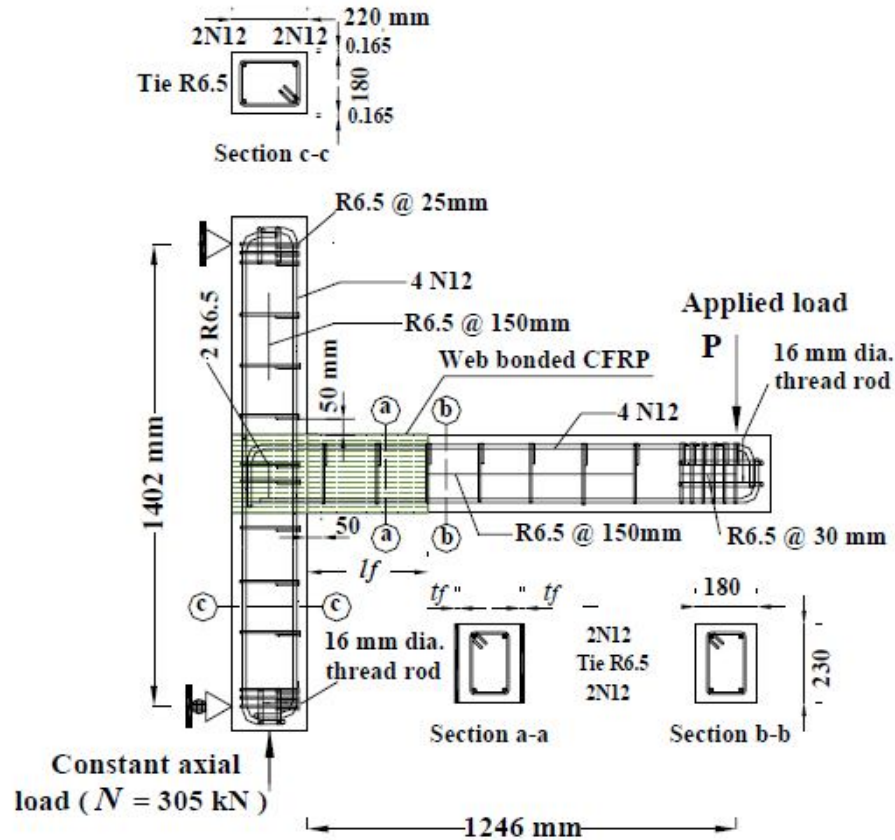


Fig. 2. Details of the selected joint [18]

The maximum loads sustained by the retrofitted specimens RSM1 and RSM2 were reported to be 24.70 kN and 21.12 kN, respectively. As it is evident, the maximum capacity of RSM1 is almost the same as that of the control specimen, CSM0. However, the maximum load capacity of specimen RSM2 is less than that of CSM0. Although three layers of FRP were used in specimen RSM2, due to insufficient length of the FRP layers, the capacity of this specimen fell short of the strength of both the control specimen and the single-layer retrofitted joint (RSM1) [18]. For RSM2 specimen, flexural cracks started to develop beyond the cut-off point of the FRP layers. The plastic hinge and yielding of longitudinal bars occurred at the end of the attached FRP sheets. The beam tip load versus displacement for specimens CSM0, RSM1 and RSM2 are compared with each other in Fig. 3.

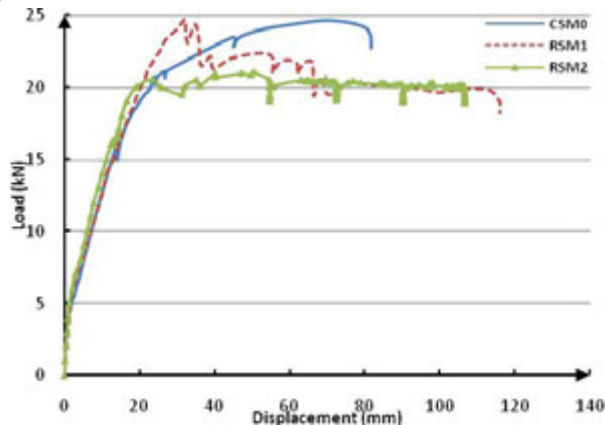


Fig. 3. Beam tip load versus displacement for CSM0, RSM1 and RSM2 [18]

### 3. NUMERICAL PROGRAM

#### a) Material and constitutive models

In the present study, the joints tested by Mahini and Ronagh were first analysed numerically using ABAQUS [25] finite element software. To achieve more accurate results, it is necessary to introduce representing material and constitutive models to the software. In the following, the constitutive models used for the concrete, steel and FRP materials are discussed.

The concrete damage plasticity (CDP) model is used to define the behaviour of concrete. The concrete damage plasticity model in ABAQUS is based on the models proposed by Lubliner et al. [31] and Lee and Fenves [32]. The CDP model can provide some useful properties including: the softening behaviour in tension as opposed to the initial hardening followed by softening in compression, different yield strengths in tension and compression, with the initial yield stress in compression being ten times more than the initial yield stress in tension [22, 23].

Hognestad stress-strain curve [33] is used to define the uniaxial compressive stress of concrete. Although there is no direct relation between the tensile and compressive strengths, a ratio of between 0.05 and 0.1 is often considered for the two strength properties [34]. Stress-strain curve of concrete under tensile stress shows little nonlinearity beyond 50 percent of tensile strength ( $0.5f'_c$ ), but in many cases it is suitable to assume that this part is also linear. The modulus of elasticity under uniaxial tension is higher and the poisson's ratio lower than in uniaxial compression. As for the modulus of rupture, ACI committee 318 [30] has proposed that  $f_r = 0.7\sqrt{f'_c}$ .

Under multiaxial stresses, however, concrete shows different behaviour from that of the uniaxial stresses. Recent studies have shown that under biaxial compression, the maximum biaxial compressive strength is approximately 16 to 25 percent higher than the uniaxial compressive strength. Also, under biaxial compression-tension, the compressive strength decreases when tensile stress is increased and under biaxial tension, the compressive strength remains almost the same [34]. ABAQUS uses yield surface of Lubliner et al. [31] and Lee and Fenves [32] to determine the behaviour of concrete and the state of failure or damage under multiaxial stress.

Steel reinforcement in concrete acts mostly as a one-dimensional member. Therefore, it is not necessary to consider the complicated behaviour of steel under multi-axial stresses [34]. For simplicity, stress-strain curve of steel under tension or compression is idealized by three straight lines with 3% strain hardening.

Mechanical properties, orientation, length, shape and composition of fibres, the mechanical properties of the resin matrix and the adhesion of the bond between the fibres and the matrix are factors which have important effects on the behaviour of FRPs. Composites in general are linear elastic to failure (although the latter occurs at large strains) without any significant yielding or plastic deformation, leading to a very low ductility. Composite materials have a failure surface by which the status of composite during the loading is defined. The orthotropic plane stress failure models can be used for any type of element that uses a plane stress formulation such as shell or membrane elements. A number of theories are proposed for the orthotropic plane stress failure. Five of the more popular theories include: the maximum stress, Tsai-Hill, Tsai-Wu and Azzi-Tsai-Hill which are stress-based theories and the maximum strain theory which is a strain-based theory [35]. Here, Tsai-Wu theory is used to introduce the failure surface of FRP composite to ABAQUS software (Fig. 4).

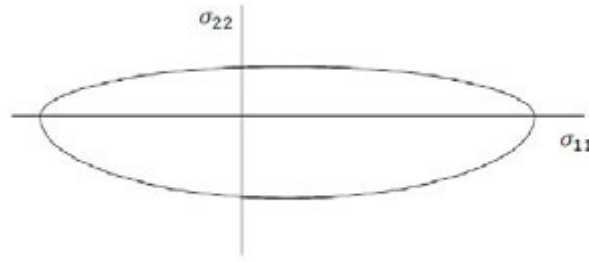


Fig. 4. Tsai-Wu failure envelope ( $I_F = 1.0, F_{12} = 0.0$ )

The Tsai-Wu failure criterion requires that;

$$I_F = F_1\sigma_{11} + F_2\sigma_{22} + F_{11}\sigma_{11}^2 + F_{22}\sigma_{22}^2 + F_{66}\sigma_{12}^2 + 2F_{12}\sigma_{11}\sigma_{22} < 1.0 \quad (1)$$

Where,

$$\begin{aligned} F_1 &= \frac{1}{X_t} + \frac{1}{X_c} & F_2 &= \frac{1}{Y_t} + \frac{1}{Y_c} \\ F_{11} &= -\frac{1}{X_t X_c} & F_{22} &= -\frac{1}{Y_t Y_c} \\ F_{66} &= \frac{1}{S^2} \end{aligned} \quad (2)$$

If the equibiaxial stress at failure  $\sigma_{biax}$  is known, then;

$$F_{12} = \frac{1}{2\sigma_{biax}^2} \left[ 1 - \left( \frac{1}{X_t} + \frac{1}{X_c} + \frac{1}{Y_t} + \frac{1}{Y_c} \right) \sigma_{biax} + \left( \frac{1}{X_t X_c} + \frac{1}{Y_t Y_c} \right) \sigma_{biax}^2 \right] \quad (3)$$

Otherwise,

$$F_{12} = f^* \sqrt{F_{11} F_{22}} \quad (4)$$

In this article  $f^*$  is assumed zero. In relations (1) to (4), 1 and 2 indices imply the material behaviour of the fibres, parallel-to-fibres and transverse-to-fibre directions, respectively;  $\sigma_{11}$  and  $\sigma_{22}$  are stress components in directions 1 and 2;  $X_t$  and  $X_c$ , are tensile and compressive stress limits in the direction 1;  $Y_t$  and  $Y_c$  are tensile and compressive stress limits in direction 2 and  $S$  is shear strength (maximum shear stress) in the X-Y plane. Also, tensile values must be positive and compressive values must be negative.

The material properties used in the analyses are  $E_1 = 240$  GPa,  $E_2 = 18581$  MPa,  $G_{12} = 12576$  MPa,  $G_{13} = 12576$  MPa,  $G_{23} = 7147$  MPa,  $X_t = 3900$  MPa,  $X_c = 80$  MPa,  $Y_t = 53.7$  MPa,  $Y_c = 80$  MPa,  $S = 42$  MPa,  $\nu_{12} = 0.2$ ,  $f^* = 0$ , in which  $E_1$  and  $E_2$  are the generalized Young's moduli in the principal directions 1 of and 2 respectively,  $G_{12}$ ,  $G_{13}$  and  $G_{23}$  are the shear moduli in the principal directions of 1, 2 and 3 respectively,  $X_t$  is the tensile stress limit in the fibre direction,  $X_c$  is the compressive stress limit in the fibre direction,  $Y_t$  is tensile stress limit in the transverse direction,  $Y_c$  is compressive stress limit in the transverse direction,  $S$  is the shear strength in the X-Y plan,  $\nu_{12}$  is the Poisson's ratio and  $f^*$  is the cross product term coefficient [36].

#### b) Verification of the numerical models

To verify the accuracy of the numerical models, the control joint CSM0 and the retrofitted joints RSM1 and RSM2 tested by Mahini and Ronagh [18] are modelled and analysed and the results are compared with those obtained from the experiments. FRP shells are considered attached to the outer

surface of concrete directly and a perfect bond between FRP and concrete is assumed. To avoid the local instability and concrete failure, a steel plate is located on the column where the constant load is applied. To model the joints, 2645 continuum 8-node linear brick elements (C3D8R) with three degrees of freedom per node and 226 two-node linear 3-D trusses (T3D2) are used to model the concrete and steel reinforcements, respectively. FRP sheets are modelled by 224, 8-node shell elements with six degrees of freedom per node (S8R). For the steel plate, located on the column, 30 linear hexahedral elements (C3D8R) are used.

In the analysis, loading of the joint was considered at two stages. In the first stage, a monotonically increasing axial load of up to 305 kN, representing the gravity load pre-compression, was applied to the column. In the second stage, the column remained subjected to the constant 305 kN axial load while a step-wise increasing displacement was applied to the tip of the beam. Numerical analyses versus experimental results for the control joint, CSM0, and the strengthened joint, RSM1, models are illustrated in Fig. 5 and Fig. 6, respectively. Numerical results for the original specimen show good agreement with experimental results. Maximum applied-load for experimental and analytical specimen is 24.6 and 23.9 kN, respectively which differ around 3.2 percent. However, during the initial part of the diagram, the results of finite element analysis of the retrofitted specimen do not correlate exactly with those from the experimental data. The finite element model has higher initial stiffness due to modelling of uncracked concrete in finite element program. Concrete joint, which is modelled in ABAQUS, is uncracked while in the experiment, load is applied to cracked and retrofitted joint. Therefore, cracks in concrete and at the interface between the cement and aggregate cause lower stiffness for the experimental specimen. Maximum load carrying capacity for the experimental and numerical RSM2 specimen is 25.89 and 25.82 kN, respectively. There is only 0.27 percent difference between experimental and analytical results.

When a concrete specimen undergoes tensile stresses it will crack along different directions and strain softening occurs in the post failure region. This defines tension softening behaviour of the concrete [34]. To reduce the effect of mesh sensitivity on the solution of the problem, ABAQUS uses Hillerburg's fracture energy [25] to define the energy which is required to open a unit area of crack,  $G_f$ , the fracture energy is the area under the failure stress-crack width curve (Fig. 7). In this figure,  $f'_{t_0}$  and  $\delta_{t_0}$  are the tensile strengths of the concrete and the maximum crack opening, respectively. With reference to Fig. 7, the fracture energy is specified as;

$$G_f = \frac{\delta_{t_0} \times f'_{t_0}}{2} \quad (5)$$

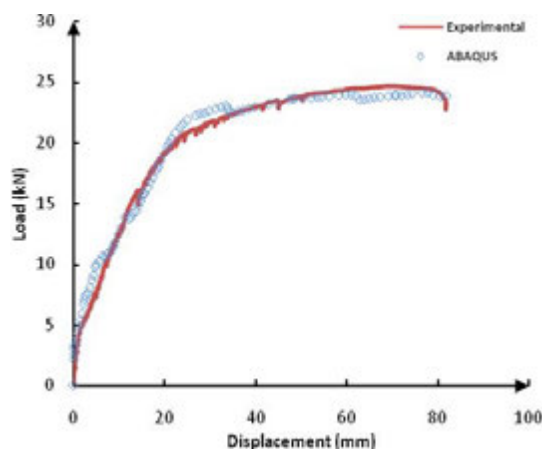


Fig. 5. Numerical versus experimental results for CSM0 specimen

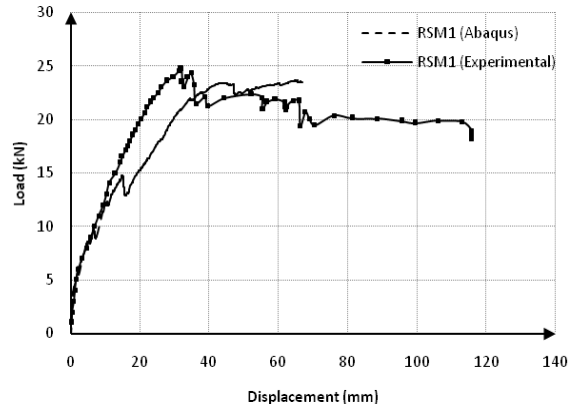


Fig. 6. Numerical versus experimental results for RSM1

Different fracture energies are chosen to study the effect of this parameter on the behaviour of the original specimen and results are presented in Fig. 8. It is evident that when fracture energy is increased, the area under load-displacement curve is increased. This increase is more noticeable in the displacement range of 2.5 to 23 mm, but after this range, the load-displacement relation obtained using different fracture energies will be almost the same. This indicates that the fracture energy parameter has negligible effects on the ultimate capacity prediction.

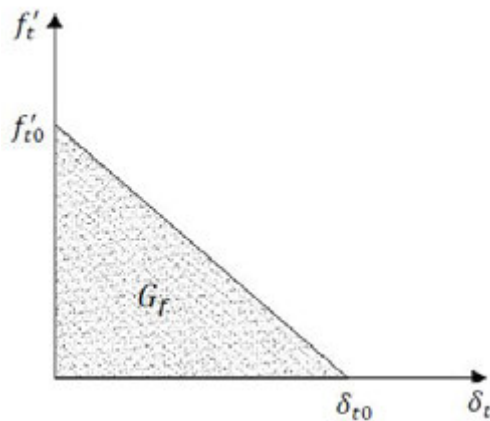


Fig. 7. The concrete tension softening

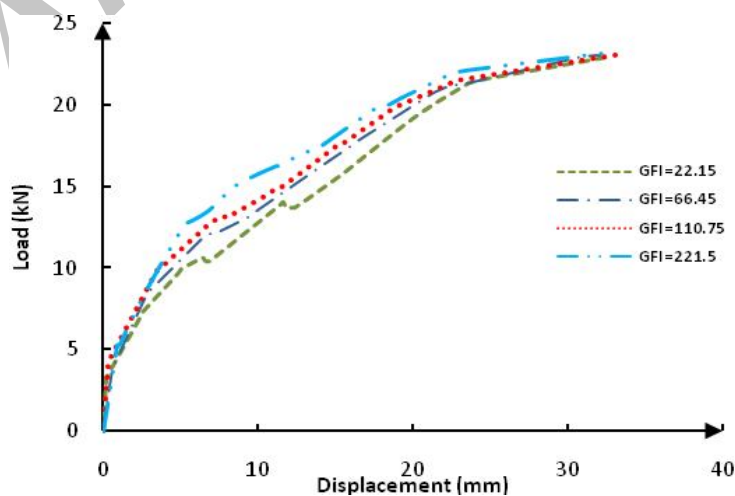


Fig. 8. Influence of different values of fracture energy on the solution



### c) The effects of length of FRP sheet

In the experimental program discussed above, the RSM2 model retrofitted with three, 200mm long layers of FRP did not perform as well as the model retrofitted with one layer but having a length of 350mm. This observation highlights the importance of the length of retrofitting FRP layers. To investigate this point numerically, the RC joint of the experiments was retrofitted with one and two layers of FRP (1LRJ and 2LRJ, respectively), both extending 350 mm from the face of the column and 1 mm thickness for each layer. According to the finite element results, the first steel yielding for original specimen occurs within the joint at 17.352 kN load, while for the 2LRJ specimen yielding of steel occurs in the beam (at the end of FRP, a distance of 350 mm from the face of the column) at 20.494 kN load, but for 1LRJ the steel yielding occurs 150 mm closer to the face of the column than the 2LRJ specimen. In addition, according to Fig. 9 cracks are developed at a distance of 90 mm from the column face for CSM0 model and at a distance of 350 mm from the column face for both 1LRJ and 2LRJ models. It is evident that for a relocation of the plastic hinge away from the column face into the beam, sufficient length of FRP layers is vital.

The thickness of the FRP layer is also an important factor for successful relocation of the plastic hinge as is evident when we compare the results of models 1LRJ and 2LRJ. Fig. 9 shows that a larger section of 1LRJ joint core has been cracked compared to the 2LRJ joint. Load-deflection curves of CSM0 and 2LRJ specimens are compared in Fig. 10.

In order to investigate the effects of FRP length on the behaviour of the joints, plain specimen (CSM0) was retrofitted by different lengths of 220, 360, 465 and 570 mm FRP sheets. As it is obvious, using longer FRP sheets, a farther yielding point is achievable. With reference to Fig. 9, it is noted that without using FRP, plastic hinges are formed too closely to the joint and this distance will be dramatically shifted into the beam using FRP with 350 mm length (nearly at the end of FRP sheets).

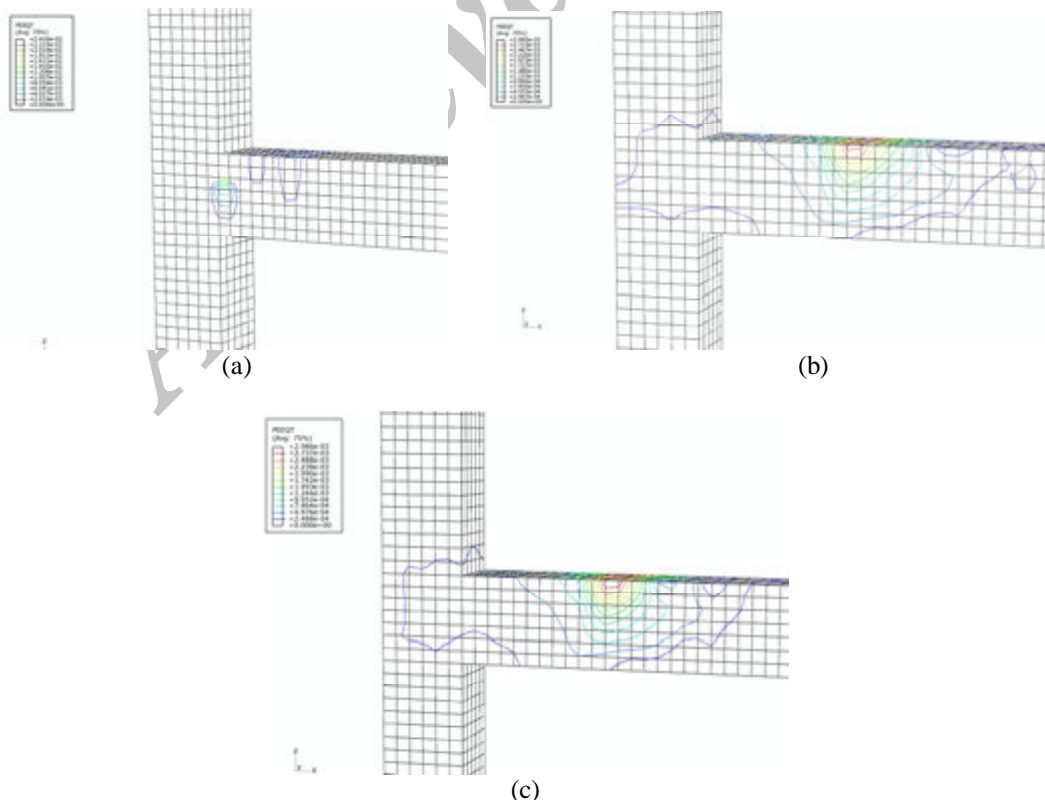


Fig. 9. Cracking pattern of (a) original, (b) 1LRJ and (c) 2LRJ

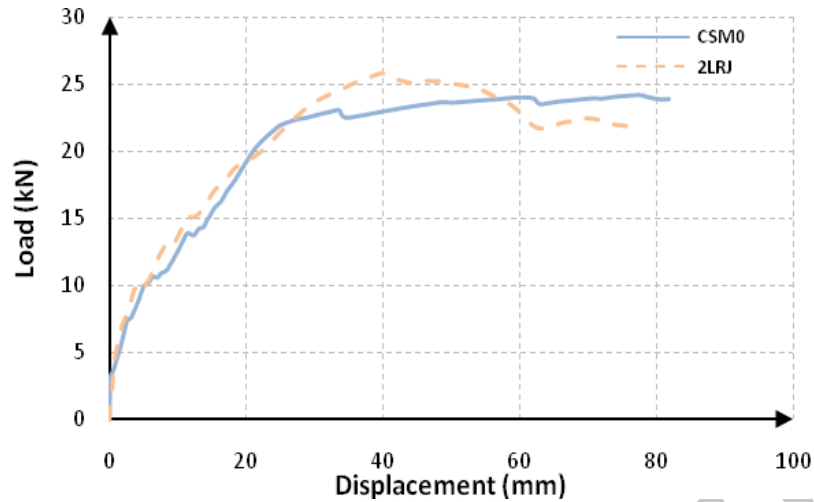


Fig. 10. Load-deflection curve of original and retrofitted joint

#### d) Pushover analysis

To study the influence of the retrofitting technique, nonlinear pushover analysis was carried out by the finite element analysis software SAP2000 [27] for both the original and the retrofitted eight-storey frames (Fig. 1). The static nonlinear procedure consists of two types of loading; (i) gravity loads which are constant during the nonlinear analysis and (ii) the lateral load which is applied at the top floor and increased monotonically.

The lateral load distribution is proportionate with the product of the storey mass and the first mode shape of the structure. Mass source of building is assumed Dead load plus 20% of Live load according to the Iranian seismic code (standard No. 2800) [37]. The P-delta effect is taken into account during the pushover analysis. Flexural moment hinges and force-moment hinges are assumed for beams and columns, respectively. Link property is used to introduce the behaviour of plastic hinges into SAP2000 software. For this purpose, full post-peak moment-rotation curves of the original and the retrofitted specimens (CSM0, 1LRJ and 2LRJ) were extracted from the joints analyses carried out using ABAQUS software (Fig. 11). It is evident that with two layers of FRP (2LRJ), the strength and stiffness of the joint are increased and the initial slope of the retrofitted joint is 28 percent higher than that of the original (plain) frame (Table 2).

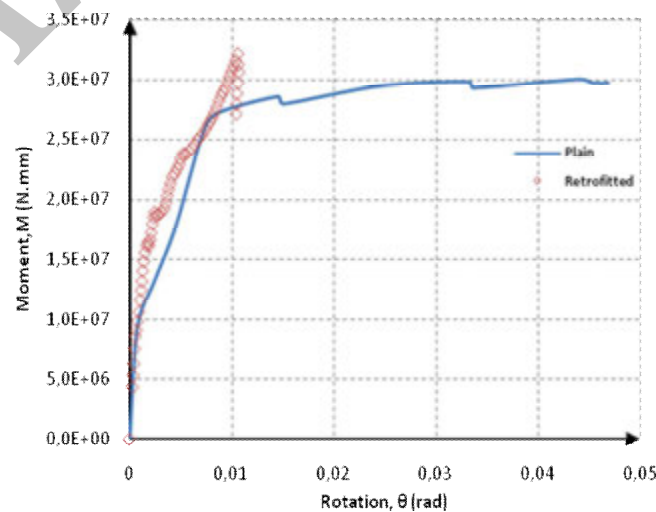


Fig. 11. Moment-rotation curve of plain (CSM0) and retrofitted (1LRJ) specimens

Base shear-roof displacement curves of the original and the retrofitted frames obtained from nonlinear pushover analysis of the original and the retrofitted frame (1LRJ) are plotted in Fig. 12. The maximum base shears for the two specimens are also compared in Table 2. Table 2 indicates that the retrofitting technique has increased the lateral load-carrying capacity of the frame by 14.6%.

Table 2. Comparison between original and retrofitted specimens

	Original specimen	Retrofitted specimen (1LRJ)	Percentage of differences (%)
Maximum moment (N.mm)	$3.01 \times 10^7$	$3.22 \times 10^7$	6.8
Initial slope of moment-rotation curve (N.mm/rad)	$12.7 \times 10^9$	$16.3 \times 10^9$	28
Ductility	6.67	4.30	-35.5
Maximum base shear (kN)	141.85	162.57	14.6
Initial slope of pushover curve (MN/mm)	3.51	3.95	12.5

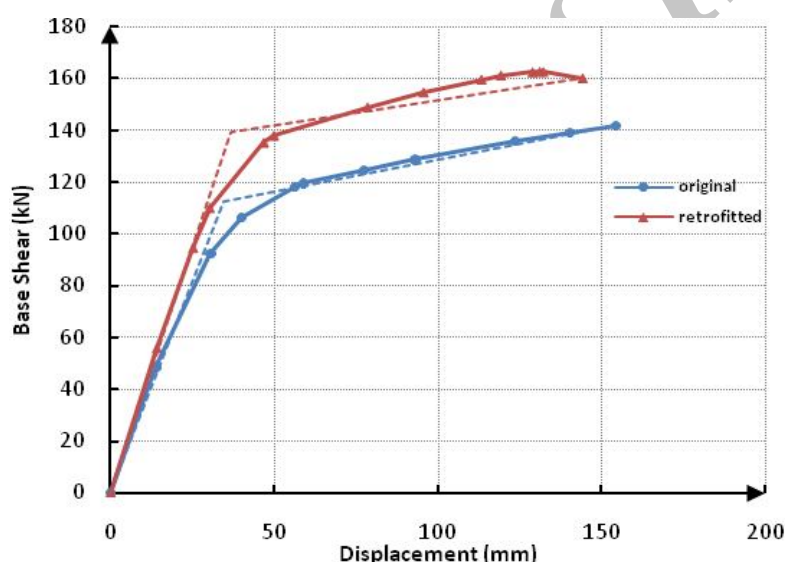


Fig. 12. Base shear-roof displacement relationship of original and retrofitted specimen

To evaluate the ductility ratios of the frames, bilinear curves are fitted to the pushover curves of the original and retrofitted frame, 1LRJ. With reference to Fig. 13, the ductility ratio,  $\mu$ , is calculated using the following relation;

$$\mu = \Delta_{max} / \Delta_y \quad (6)$$

where,  $\Delta_{max}$  is the ultimate displacement and  $\Delta_y$  is the idealized structural yield displacement evaluated from the bilinear curve using FEMA-273 [38]. Based on the bilinear curves, ductility ratio of the retrofitted frame decreased by 11.71% compared to the original frame (Table 2). This is because of the brittle behaviour of FRP causing a reduction in ductility of the retrofitted joints.

#### e) R factors of the frames

The behaviour factor,  $R$ , which in some codes is called response modification factor, is a force reduction factor used to reduce the linear elastic response spectra to the inelastic response spectra [39, 40].

This factor consists of three different components (Eq. (7)); the ductility reduction factor ( $R_\mu$ ), the overstrength factor ( $R_s$ ) and the allowable stress factor ( $Y$ ).

$$R = R_\mu \cdot R_s \cdot Y \quad (7)$$

In this article,  $R_\mu$  is determined by a relation presented by Nassar and Krawinkler [41]. Because of using the ultimate strength method, the allowable stress factor,  $Y$ , is assumed unity and  $R_s$  is evaluated as;

$$R_s = \frac{V_y}{V_s} \quad (8)$$

where,  $V_y$  is the idealized yield strength and  $V_s$  is the base shear at which the first plastic hinge is formed in the structure (Fig. 13). These seismic behaviour parameters, calculated for both the original and the retrofitted frames, are presented in Table 3. Results as presented in Table 3 show that although FRP retrofitting of joints somewhat reduces ductility, it does not have a great effect on the behaviour factor,  $R$ .

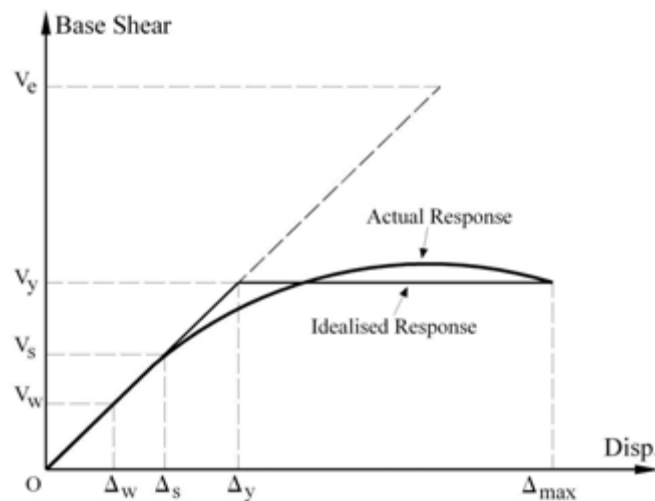


Fig. 13. Idealised bi-linear model of the pushover curve for calculation of earthquake response parameters

Table 3. Seismic behaviour parameters of original and retrofitted structures

	T (sec)	$\Delta_u$ (mm)	$V_u$ (kN)	$\Delta_y$ (mm)	$V_y$ (kN)	$\mu$	$R_\mu$	$R_s$	R
Original frame	1.1	154.24	141.85	34.75	112.37	4.44	5.21	1.21	6.3
Retrofitted (1LRJ)	1.06	144.35	160.12	36.82	139.47	3.92	4.39	1.27	5.58
Percentage of increase (%)	-3.64	-6.41	12.88	5.96	24.12	-11.71	-15.74	4.96	-11.43

#### f) Performance levels of the frames

To evaluate the earthquake performance of the frame before and after retrofitting, the performance points of the two frames are calculated by the Capacity Spectrum Method (CSM) of ATC-40 [42]. This method estimates the maximum response of a structure by expressing both structure capacity and the ground motion demand in terms of spectral acceleration and displacement [43]. For this purpose, the base shear-roof displacement curve ( $V-\Delta$ ) should first be converted to an equivalent capacity curve in the form

of spectral acceleration versus spectral displacement ( $S_a-S_d$ ). Next, a demand spectrum should be obtained at 5% damped response spectrum. Usually the 5% damped response spectrum is in terms of spectral acceleration versus period ( $S_a-T$ ) which again should be converted to an Acceleration-Displacement Response Spectra (ADRS) format. After formation of demand spectrum in ADRS format, this demand curve should be reduced. This process is carried out by two spectral reduction values, which are applied to the constant velocity and acceleration range of spectrum [42]. Finally, both demand and capacity spectra are plotted in the same coordinates system ( $S_a-S_d$ ). Intersection point of demand and capacity spectra in ADRS format determines the performance point of the structure.

To determine the performance point of the eight-storey frame, response spectrum of the Iranian seismic code [37] is used for a region with low risk of earthquake corresponding to DBA=0.2g. Procedure A from ATC-40 is employed to reach a solution for the approximation and find the performance point of the two frames. Fig. 14 and Fig. 15 show the capacity and the seismic demand spectra in ADRS format for the original frame and the ILRJ retrofitted frame, respectively. As it is seen in Fig. 14, the original frame cannot satisfy the performance level required by the design earthquake and it has no performance point in relation to the design earthquake demand. However, the retrofitted frame has a performance point with coordinates (12.27, 0.126g) (Fig. 15). Roof displacement at performance point for retrofitted specimen is 156.9 mm. According to FEMA 356 [38], the limitation of displacement for life safety performance level of reinforced concrete frames is 1% to 2% of the height of the building (120.2 mm to 240.3 mm). Therefore, retrofitted frame meets the performance objectives of life safety. According to these results, this retrofitting technique can improve the behaviour of the frame under earthquake motions to the desired level. It should be noted that response spectrum of standard 2800 is much higher than the response spectrum of the Australian standard [44], because earthquake hazard in Australia is lower than that in Iran.

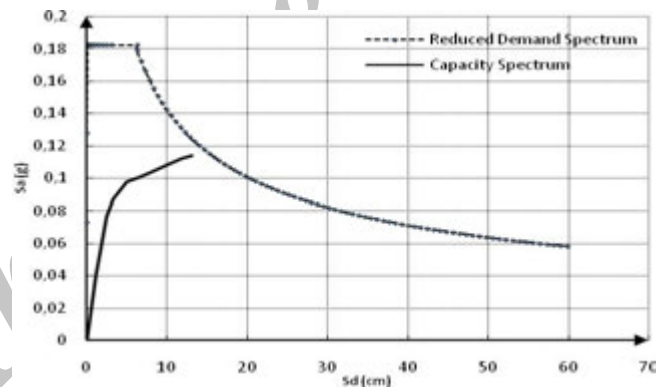


Fig. 14. The capacity and the seismic demand spectra in ADRS format for the original frame

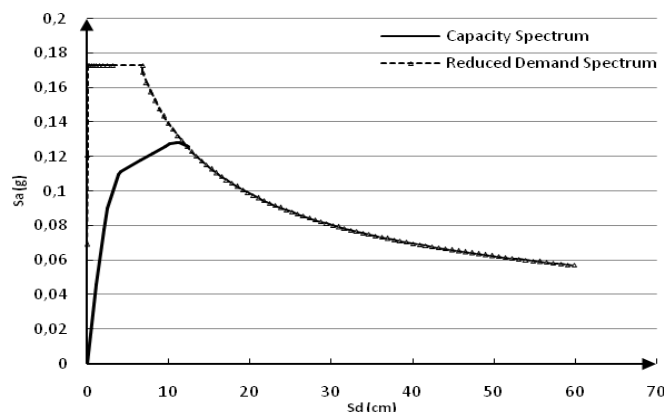


Fig. 15. The capacity and the seismic demand spectra in ADRS format for the retrofitted (ILRJ) frame

**g) Seismic performance of low-rise frames retrofitted with FRP and X-steel braces**

To study the seismic behaviour of low-rise buildings retrofitted by FRP materials and by steel braces, based on the works carried out on steel bracing of RC frames by Maheri et al [45-47], two ordinary moment resisting frames were investigated; a 2-storey and a 4-storey frame (Fig. 16). In the case of retrofitting by steel braces, braces were placed in the middle bay of the frames. For FRP retrofitting technique, all the joints except the joints of the last floor were retrofitted on their web by FRP sheets. Vertical gravity loads were derived from the Iranian code and calculated as D.L. = 2200 kg/m and L.L. = 1400 kg/m. Equivalent static earthquake lateral loads on the frames were calculated using design response spectrum of the Iranian seismic code [37].

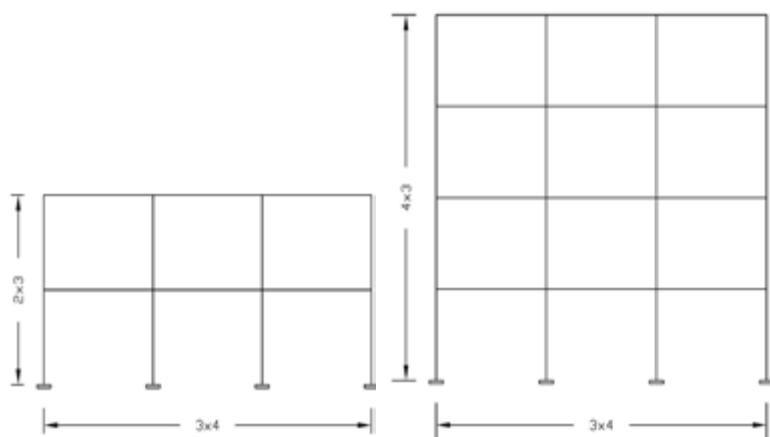


Fig. 16. Geometry of studied frames

To evaluate the seismic load it was assumed that the frames are located in a zone with high seismic hazard ( $DBA = 0.35g$ ). At first, the seismic reduction factor was assumed to be  $R=4$  and 75% of the lateral load ( $0.75V$ ) was applied to design each RC frame. However, after adding X-steel braces to the RC frames, 100% of the lateral load was applied ( $V$ ). Therefore, steel braces were designed to undergo 25% share of the lateral load. The braces were then designed according to AISC-LRFD 93 code of practice [48]. To design the RC members of frames by SAP2000 program [27], load combinations of ACI318-99 [49] were used.

Compressive strength of concrete and yield stress of steel reinforcements was assumed to be  $40 \text{ N/mm}^2$  and  $340 \text{ N/mm}^2$ , respectively. For all sections, minimum and maximum values of steel reinforcements were checked based on Iranian Concrete Code (ABA) [50].

Nonlinear, pushover analyses were carried out on the 2-storey and 4-storey frames before and after retrofitting by FRP materials at joints and X-steel braces. For this purpose, the joints were first modelled in ABAQUS finite element program and moment-rotation curve for each joint was evaluated. The moment-rotation relation of the joints was then incorporated in the FE models of the frames and pushover analyses were carried out using SAP2000 program. Figures 17 and 18 present base shear-roof displacement curves for the 2-storey and the 4-storey frames, respectively, obtained from the pushover analyses. The base shear roof displacement curve for the 2-storey and 4-storey frame retrofitted by steel bracing is also shown in Fig. 17 and Fig. 18, respectively. Figures 17 and 18 show that the shear capacity of frames increases, using both FRP joint web-bonding and steel bracing systems; as expected, the steel bracing is capable of increasing the strength of the frames to much higher levels than the FRP joint web-bonding. When frames are retrofitted with the X-steel braces, the stiffness of the system is also increased considerably. However, ductility and behaviour factor of the FRP-retrofitted frames appear to be more than those of the steel bracing as quantified in Table 4.

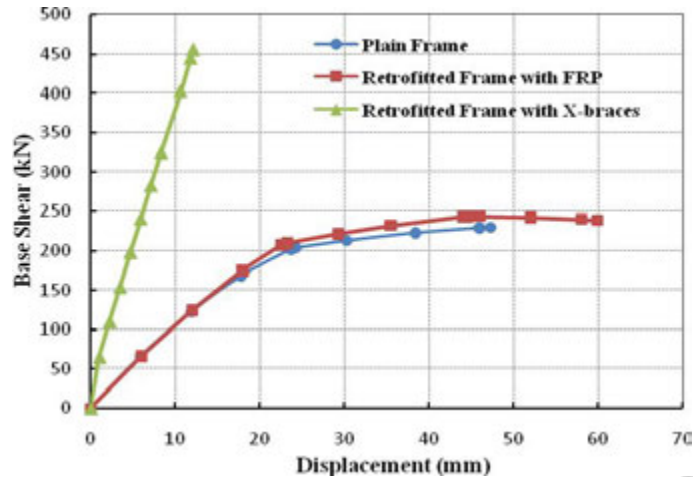


Fig. 17. Pushover results of 2-storey frame

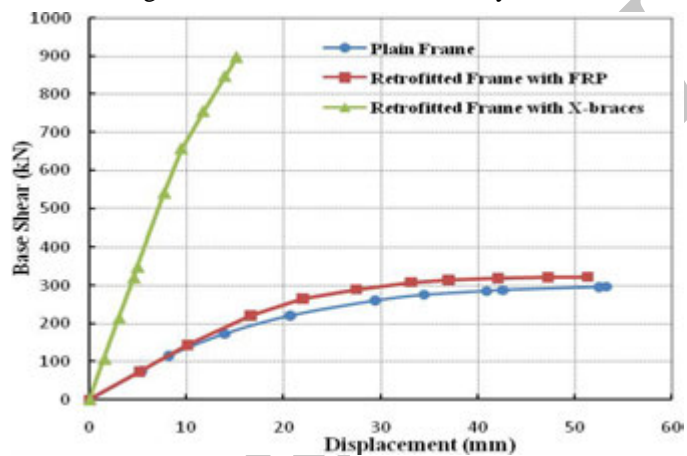


Fig. 18. Pushover results of the 4-storey frame

Table 4. Seismic parameters of 2-storey and 4-storey frames

No. of Stories	Type of frames	T	$R_{\mu}$	$R_s$	R
2	Plain frame	0.44	2.38	1.69	4.02
	Retrofitted by FRP	0.44	2.55	1.96	4.99
	Retrofitted by X-braces	0.2	1.2	3.65	4.37
4	Plain frame	0.56	3.05	1.49	4.54
	Retrofitted by FRP	0.56	2.58	1.99	5.14
	Retrofitted by X-braces	0.25	1.46	3.4	4.96

The seismic behaviour parameters including: the ductility reduction factor, overstrength factor and the behaviour factor for the 2-storey and 4-storey frames, before and after retrofitting by FRP and X-steel braces, were calculated using base shear-roof displacement capacity curves of the frames.

According to Table 4, by using X-steel braces, fundamental periods of frames reduce. This is due to the higher stiffness provided by the steel bracing. Also, X-steel braces expectedly exhibit higher overstrength and reduced ductility, whereas FRP retrofitting of joints provides higher ductility as well as higher overstrength. The behaviour factor,  $R$ , as the product of the two parameters is also higher for the FRP joint retrofitting compared to the steel bracing of the frames. The  $R$ -factor differences for the frames retrofitted by FRP layers and X-steel braces are 14.2% and 3.63% for the 2-storey and 4-storey frames, respectively. It seems that the difference in  $R$ -factor reduces with increasing number of stories. In other

words, FRP joint retrofitting is more effective for shorter frames, whereas steel bracing appears more suitable for taller frames.

Earthquake performance points of the original and the retrofitted frames were also calculated using the CSM method of ATC-40 [42]. Table 5 presents performance points of the frames. According to this Table, the 4-storey frame retrofitted by FRP laminates at joints has no performance point. This may be due to insufficient layers of FRP materials. The load capacity and the performance of the frame can be enhanced using thicker layers of FRP. The X-brace retrofitted frames, however, have performance points meeting the life safety requirements.

Table 5. Performance points of the original and retrofitted frames

Type of frame	Performance point	
	2-storey	4-storey
Plain	(4.00 , 0.36g)	(2.66 , 0.27g)
Retrofitted with FRP laminates	(3.79 , 0.38g)	N.A.
Retrofitted with X-braces	(1.00 , 0.70g)	(0.92 , 0.66g)

#### 4. CONCLUSION

In this paper, nonlinear pushover analyses are carried out to evaluate the behaviour of RC joints retrofitted on the web by FRP laminates and of full-scale RC frames retrofitted at joints only by FRP composite layers. Based on the results of these analyses the following conclusions may be drawn.

- The beam plastic hinging zone, where excessive cracks may occur, is successfully relocated away from the face of the column to the end of FRP laminates inside the beam when the joint is web-bonded by FRP sheets with sufficient thickness and length.
- To investigate the influence of joint FRP-web bonded technique, pushover analyses were carried out on an eight-storey frame. Results indicate that this retrofitting method not only maintains the lateral load-carrying capacity of the damaged frame, but also increases its seismic performance. The maximum capacity of the retrofitted frame increased by 14.6 percent. However, because of the reduction in FRP-bonded joints' ductility, ductility ratio of the retrofitted structure was reduced by 11.71%.
- According to pushover analyses results, the behaviour factor,  $R$ , is increased by 10.66% when the frame was retrofitted at joints by two layers of FRP laminates. Further increases in both the lateral load capacity and the behaviour factor may be achieved by using thicker layers of FRP.
- It was shown that the original frame could not satisfy the performance demand of the Iranian seismic code. Considering that the original frame was designed according to the Australian seismic code, the shortfall of the frame is explained by the differences between the Iranian and the Australian response spectra. However, the FRP-retrofitting of the joints upgraded the frame to satisfy the life safety performance level of the Iranian code.
- According to the results of the 2-storey and 4-storey frames, both the behaviour factor and the base shear capacity of the joint web-bonded FRP-retrofitted frames showed improvements compared to the original frames. However, the FRP-retrofitting of the 4-storey frame failed to upgrade the frame to satisfy the life-safety performance demand of the selected Iranian design earthquake, indicating insufficient thickness considered for the FRP laminates. The steel bracing of the frames, on the other hand, considerably enhanced their performance to meet the required life-safety demands, by substantially increasing capacities of the frames at the expense of highly reduced ductility.



## REFERENCES

1. Flexural Retrofit of Rectangular Reinforced Concrete Bridge Columns by Steel Jacketing: Experimental Studies. Report No. SSRP-93/01. Department of Applied Mechanics and Engineering Sciences, University of California at San Diego, San Diego, CA, USA. 215.
2. Biddah, A., Ghobarah, A. & Aziz, T. S. (1997). Upgrading of nonductile reinforced concrete frame connections. *Journal of Structural Engineering, ASCE*, Vol. 123, No. 8, pp. 1001-10.
3. Alcocer, S. M. & Jersa, J. (1993). Strength of reinforced concrete frame connections rehabilitated by jacketing. *ACI Structural Journal (American Concrete Institute, Detroit, MI, USA)*, Vol. 90, No. 3, pp. 249-61.
4. Kuan, S. Y. W. (1991). Response of epoxy-repaired R/C exterior beam-column joints. *Proceedings of 1991 Annual Conference of Canadian Society for Civil Engineering*. Vancouver, BC, Canada, pp. 335-344.
5. Filiatrault, A. & Lebrun, I. (1996). Seismic rehabilitation of reinforced concrete joints by epoxy pressure injection technique. in *Seismic Rehabilitation of Concrete Structures*, SP-160, American Concrete Institute, Farmington Hills, pp. 73-92.
6. Varastehpour, H. & Hamelin, P. (1997). Strengthening of concrete beams using fiber-reinforced plastics. *Material and Structures*, Vol. 30, pp. 160-166.
7. Kachlakev, D. & McCurry, D. D. (2000). Behavior of full-scale reinforced concrete beams retrofitted for shear and flexural with FRP laminates. *Composites: Part B*, Vol. 31, pp. 445-452.
8. Almusallam, T. H. & Al-Salloum, Y. A. (2001). Ultimate strength prediction for RC beams externally strengthened by composite materials. *Composites: Part B*, Vol. 32, pp. 609-619.
9. Sheikh, S. A. (2002). Performance of concrete structures retrofitted with fiber reinforced polymers. *Engineering Structures*, Vol. 24, pp. 869-879.
10. Hu, H. T., Lin, F. M. & Jan, Y. Y. (2004). Nonlinear finite element analysis of reinforced concrete beams strengthened by fiber-reinforced plastics. *Composite Structures*, Vol. 63, pp. 271-281.
11. Li, j., Samali, B., Ye, L. & Bakoss, S. (2002). Behaviour of concrete beam-column connections reinforced with hybrid FRP sheet. *Composite Structures*, Vol. 57, pp. 357-365.
12. Mosallam, A. S. (2000). Strength and ductility of reinforced concrete moment frame connections strengthened with quasi-isotropic laminates. *Composites: Part B*, Vol. 31, pp. 481-497.
13. Parvin, A. & Granata, P. (2000). Investigation on the effects of fiber composites at concrete joints. *Composites: Part B*, Vol. 31, pp. 499-509.
14. Granata, P. J. & Parvin, A. (2001). An experiment study on kelvar strengthening of beam-column connections. *Composite Structures*, Vol. 53, pp. 163-171.
15. Said, A. M. & Nehdi, M. L. (2004). Use of FRP for RC frames in seismic zones: Part I. Evaluation of FRP beam-column joint rehabilitation techniques. *Applied Composite Materials*, Vol. 11, pp. 205-226.
16. Mukherjee, A. & Joshi, M. (2005). FRPC reinforced concrete beam-column joints under cyclic excitation. *Composite Structures*, Vol. 70, pp. 185-199.
17. Parvin, A. & Wu, S. (2008). Ply angle effect on fibber composite wrapped reinforced concrete beam-column connections under combined axial and cyclic loads. *Composite Structures*, Vol. 82, pp. 532-538.
18. Mahini, S. S. & Ronagh, H. R. (2010). Strength and ductility of FRP web-bonded RC beams for the assessment of retrofitted beam-column joints. *Composite Structures*, Vol. 92, No. 6, pp. 1325-1332.
19. Mahini, S. S. & Ronagh, H. R. (2009). Numerical modelling of FRP strengthened RC beam-column joints. *Structural Engineering & Mechanics*, Vol. 32, No. 5, pp. 649-665.
20. Balsamo, A., Colombo, A., Manfredi, G., Negro, P. & Prota, A. (2005). Seismic behavior of a full-scale RC frame repaired using CFRP laminates. *Engineering Structures*, Vol. 27, No. 27, pp. 769-780.

21. Zou, X. K., Teng, J. G., De Lorenzis, L. & Xi, S. H. (2007). Optimal performance-based design of FRP jackets for seismic retrofit of reinforced concrete frames. *Composites: Part B*, Vol. 7, pp. 584-597.
22. Mahini, S. S., Ronagh, H. R. & Niroomandi, A. (2008). Performance based assessment of FRP-retrofitted existing RC frames. *Proceedings of Fourth International Conference on FRP Composites in Civil Engineering (CICE08)*, Zurich, Switzerland Empa, Duebendorf, Paper 6.B.6. p. 6 (CD-ROM).
23. Niroomandi, A. Maheri, A., Maheri, M. R. & Mahini, S. S. (2010). Seismic performance of ordinary RC frames retrofitted at joints by FRP sheets. *Engineering Structures*, Vol. 32, No. 8, pp. 2326-2336.
24. Mostofinejad, D. & Talaeitaba, S. B. (2006). Finite element modelling of RC connections strengthened with FRP laminates. *Iranian Journal of Science and Technology, Transaction B: Engineering*, Vol. 30, No. B1, pp. 21-30.
25. Hibbitt, Karlsson, & Sorensen, (2007). Inc. *ABAQUS theory manual, User manual and example Manual*. Version 6.7.
26. Mahini, S. S., Hadigheh, S. A. & Maheri, M. R. (2010). Seismic assessment of FRP-retrofitted RC frames using pushover analysis considering strain softening of concrete. *Proceedings of the Fifth International Conference on FRP Composites in Civil Engineering (CICE 2010)*, Beijing, China.
27. CSI. (2007). *SAP2000 software, non-linear version 11.0.0, computers and structures*. Inc., Berkeley, California, USA.
28. Maheri, M. R. & Ghaffarzadeh, H. (2008). Connection overstrength in steel-braced RC frames. *Engineering Structures*, Vol. 30, No. 7, pp. 1938-1948.
29. AS3600, (2001). *Concrete structures*. Standards Australia, Homebush Bay, Australia.
30. ACI Committee 318, (2002). *Building code requirements for structural concrete*. American Concrete Institute, Detroit, MI.
31. Lubliner, J., Oliver, J., Oller, S. & Oñate, E. (1989). A plastic-damage model for concrete. *International Journal of Solids and Structures*, Vol. 25, pp. 299-329.
32. Lee, J. & Fenves, G. L. (1998). Plastic-damage model for cyclic loading of concrete structures. *Journal of Engineering Mechanics*, Vol. 124, No. 8, pp. 892-900.
33. Park, R. & Paulay, T. (1975). *Reinforced concrete structures*. New York: John Wiley and Sons, Inc.
34. Chen, W. F. (1982). *Plasticity in reinforced concrete*. McGraw-Hill, Inc.
35. Lundqvist, J., Nordin, H., Taljsten, B. & Olofsson, T. (2005). Numerical analysis of concrete beams strengthened with CFRP-A study of anchorage lengths. *The International Symposium on Bond Behavior of FRP in Structures (BBFS)*, Chen and Teng (eds), International Institute for FRP in Construction.
36. Mahini, S. S. & Ronagh, H. R. (2006). Computer model for repaired RC beams using web-bonded FRP sheets. *Proceeding of the Second International Conference on Concrete Repair, Concrete Solutions*, St-Malo, France, pp. 115-122.
37. Standard No. 2800, (2005). *Iranian code of practice for seismic resistant design of buildings*. Building and Housing Research Center, Third edition.
38. Federal emergency management agency (FEMA). (1997). *NEHRP provisions for the seismic rehabilitation of buildings*. Rep FEMA 273 and 274, Washington DC.
39. Maheri, M. R. & Akbari, R. (2003). Seismic behaviour factor,  $R$ , for steel X-braced and knee-braced RC buildings. *Engineering Structures*, Vol. 25, No. 12, pp. 1505-1513.
40. Akbari, R. & Maheri, M. R. (2011). 'Analytical investigation of response modification factor,  $R$ , for RC frames rehabilitated by steel chevron bracing'. *Structure and Infrastructure Engineering*. iFirst Article, 1-9.
41. Nassar, A. A. & Krawinkler, H. (1991). Seismic demands for SDOF and MDOF systems. Report No. 95. Stanford, California: The John A. Blume Earthquake Engineering Center, Stanford University.
42. ATC-40, (1996). *Seismic evaluation and retrofit of concrete buildings*. Applied Technology Council, Redwood City.

43. Barros, R.C. & Almeida, R. (2005). Pushover analysis of asymmetric three-dimensional building frames. *Journal of Civil Engineering and Management*, Vol. XL, No. 1, pp. 3-12.
44. AS1170.4, (1993). Structural design actions part 4: Earthquake actions in Australia.
45. Maheri, M. R. & Sahebi, A. (1997). The use of steel bracing in reinforced concrete frames. *Engineering Structures*, Vol. 19, No. 12, pp. 1018-24.
46. Maheri, M. R., Kousari, R. & Razzazan, M. (2003). Pushover tests on steel X-braced and knee-braced RC frames. *Engineering Structures*, Vol. 25, No. 13, pp. 1697-1705
47. Maheri, M. R. & Hadjipour, A. (2003). Experimental investigation and design of steel brace connection to RC frame. *Engineering Structures*, Vol. 25, No. 13, pp. 1707-1714.
48. *Manual of steel construction, load and resistance factor design*. (1994). LRFD. 2nd ed. American Institute of Steel Construction, Chicago, III.
49. ACI318, (1999). Building code requirements for structural concrete. American Concrete Institute.
50. ABA. (2005). Iranian concrete code. Report No. 120, Islamic Republic of Iran Management and Planning Organization.

Archive of SID